

Pressureless sintering and mechanical properties of mica glass–ceramic/Y-PSZ composite

M. Montazerian^a, P. Alizadeh^{a,*}, B. Eftekhari Yekta^b

^a School of Engineering, Tarbiat Modares University, Tehran, Iran

^b Ceramic Division, Department of Materials, Iran University of Science and Technology, Tehran, Iran

Received 5 January 2008; received in revised form 14 April 2008; accepted 18 April 2008

Available online 10 June 2008

Abstract

Mica glass–ceramic composites toughened by 5, 10 and 15 wt.% partially stabilized zirconia (Y-PSZ) were prepared via pressureless sintering. Sinterability of composites was investigated in the temperature range of 1060–1170 °C using soaking time of 240 min. The sintered specimens were characterized by scanning electron microscopy (SEM) and X-ray diffraction (XRD) methods. The results revealed that during sintering, the dissolution of Y-PSZ occurred in the residual glass which caused the formation of zircon and transformation of tetragonal to monoclinic zirconia. Mechanical properties of the sintered samples such as bending strength, Vickers micro-hardness and fracture toughness were also investigated. Measurements showed that addition of 15 wt.% ZrO₂ to the mica glass–ceramic matrix increased the bending strength from 50.91 ± 10.50 to 132.47 ± 13.80 MPa. Fracture toughness was also improved up to 1.37 ± 0.14 MPa m^{1/2}.

© 2008 Elsevier Ltd. All rights reserved.

Keywords: Glass–ceramics; Composites; Sintering; Mechanical properties; ZrO₂

1. Introduction

Mica-based glass–ceramics are well-known machinable ceramics, which have excellent thermal, electrical and biological properties. These outstanding properties make them suitable for use in high-performance applications such as aerospace industry, insulators, welding tools, biomedical applications, etc. Nevertheless, they suffer from their low hardness and insufficient mechanical strength.^{1,2} Numerous attempts have been made to overcome the mentioned weakness of these materials. The substitution of K⁺ or Na⁺ as the interlayer ions of mica crystals by Ba²⁺ or Ca²⁺ ions resulted in the formation of high-strength mica glass–ceramics.³ Orientated mica glass–ceramics fabricated by hot-pressing or extrusion processes represent high strength and toughness in comparison with the conventional mica glass–ceramics containing randomly orientated mica crystals with the house of cards structure.^{4–6} Also, they could be reinforced with zirconia (ZrO₂), which is crystallized from the

bulk glass.^{7,8} It has been reported that calcium mica-based nanocomposite, which contains nano-size (20–50 nm) tetragonal ZrO₂ particles, exhibits high flexural strength and fracture toughness.⁷ The excellent mechanical performance is related to crack deflection by mica plates and phase transformation of ZrO₂ particles.^{7,8} It should be noted that all these researches have been done on mica glass–ceramics fabricated via melt-cast method, and there are a few work done on the sintering process.^{9–11} Previous study revealed that by using an additive such as P₂O₅, viscous flow sintering can be successfully used to produce mica glass–ceramic with excellent machinability and appropriate final density. Optimum composition obtained from the sintering method was selected as a matrix of composite in this study.⁹

Zirconia is a very important ceramic for its transformation-toughening behavior. It goes through a martensitic phase transformation from tetragonal-to-monoclinic by a thermal hysteresis loop, since it occurs at about 1150 °C during heating (monoclinic-to-tetragonal) and at about 950 °C during cooling (tetragonal-to-monoclinic).¹² It is well-known that the stress-induced transformation of metastable tetragonal ZrO₂ to monoclinic ZrO₂ consumes the energy of propagating crack and

* Corresponding author at: School of Engineering, Tarbiat Modares University, P.O. Box 14115-143, Tehran, Iran. Tel.: +98 21 88011001.

E-mail address: p-alizadeh@modares.ac.ir (P. Alizadeh).

stop it from further propagation. To extend the crack further requires additional tensile stress. The result of this behavior is a ceramic that is very tough, strong and suitable for use as a reinforcement in the matrix of composites.^{13,14}

In this study, in order to improve mechanical properties, mica glass–ceramic composites toughened by partially stabilized zirconia particles (Y-PSZ, ZrO₂ stabilized with 3 mol% Y₂O₃) were synthesized by employing pressureless sintering. Additionally, microstructural studies and investigation into the toughening mechanisms of the composite were the objectives of this work.

2. Experimental procedure

The theoretical composition of mica-based glass was 40.13 wt.% SiO₂, 16.24 wt.% Al₂O₃, 19.11 wt.% MgO, 8.00 wt.% K₂O, 2.23 wt.% B₂O₃, 9.55 wt.% F and 4.45 wt.% P₂O₅. The raw materials used in the preparation of glass were all high quality reagents of SiO₂, Al₂O₃, Mg(OH)₂, K₂CO₃, H₃BO₃, MgF₂ and NH₄H₂PO₄. The thoroughly mixed glass batch (~200 g) was preheated at 900 °C for 1 h and then melted in platinum crucible at 1410 °C for 30 min. The melt was then quenched in cold distilled water to obtain frit.

Then the frit was milled in a high-speed alumina mill in an ethanol environment for 45 min. The particle size measurement of the glass powder was carried out by a laser particle size analyzer (Fritsch, Analysette 22).

The milled glass powder was mixed with 5, 10 and 15 wt.% Y-PSZ powder (Aldrich; submicron powder with mean particle size of 0.89 μm). Wet mixing in ethanol was performed for 6 h in an alumina jar-mill. The dried powder of each sample was granulated by adding 2 wt.% polyvinyl alcohol solution.

The granulated powders were pressed using a uniaxial hydraulic press into discs (10 mm in diameter and 4 mm thickness) at a final pressure of 65 MPa. After the organic binder was removed from the samples by holding at 450 °C for 1 h, the discs were fired between 1060 and 1170 °C, in an electric furnace. The heating rate was 20 °C/min and the sample remained in the maximum temperature for 240 min. The mica glass–ceramic named as Mica, and the composites containing 5, 10 and 15 wt.% Y-PSZ here-after are referred to as M5Z, M10Z and M15Z, respectively.

The bulk density of sintered samples was determined by Archimedes method. The crystallized samples were then subjected to X-ray diffraction (XRD) analysis using a powder diffractometer (Siemens D-500, Cu K α radiation at 40 kV). The microstructural studies were done by scanning electron microscope (SEM, Philips XL30). The content of tetragonal zirconia phase was determined using the method of Garvie and Nicholson.¹⁵

Sintered rectangular bars (2.5 mm × 5 mm × 25 mm) were also used for three-point bending strength and fracture toughness measurements.

The fracture strength measurements were performed on single edge-notched bar (SENB) specimens with a span of 20 mm, and a nearly half-thickness notch (~2.5 mm) was made using a low speed diamond cutting saw (Buehler, Isomet). The notch had a nominal thickness of 0.3 mm. The fracture toughness value was

calculated according to ASTM E399. The flexural strength and the fracture toughness measurements of the glass–ceramic and composites were conducted in air at room temperature (Instron Universal Testing Machine-1196) with a crosshead speed of 1 mm/min. At least seven specimens were tested for each series of composition. A Vickers micro-hardness tester with a diamond pyramid indenter (Buehler, Micromet 1) was used to measure micro-hardness. The load was 500 g and the loading time was 30 s. Data of hardness were determined using at least 10 indentations on each polished specimen.

3. Results and discussion

Fig. 1 shows the particle size distribution of the glass powder, which has a mean particle size of 12.5 μm. Calculated relative density of green compacted specimens was 56% for glass powder, 54% for M5Z and 51% for M10Z and M15Z.

Relative densities of the specimens versus firing temperatures are plotted in Fig. 2. By increasing the temperature, relative density increased to the maximum values and then decreased at higher temperatures. Achieving the maximum density was a criterion for determining the optimum sintering temperatures. Therefore, the temperatures of 1100, 1110, 1120 and 1130 °C were chosen for Mica, M5Z, M10Z and M15Z as the optimum sintering temperature, respectively. As it was expected, adding Y-PSZ particles into the glass–ceramic matrix reduced the sinterability and increased the sintering temperatures of specimens. Bloating of the samples caused a decrease in the relative densities of them, when excessive sintering temperatures were employed. Bloating of the specimens can be attributed to the volatilization of silicon tetrafluoride at the final stage of sintering when the open porosities are now closed.

XRD patterns of the sintered mica glass–ceramic and the composites are shown in Fig. 3. The sintered glass–ceramic contained fluorophlogopite, forsterite and spinel (MgAl₂O₄). Besides the mentioned phases, monoclinic zirconia (m-ZrO₂),

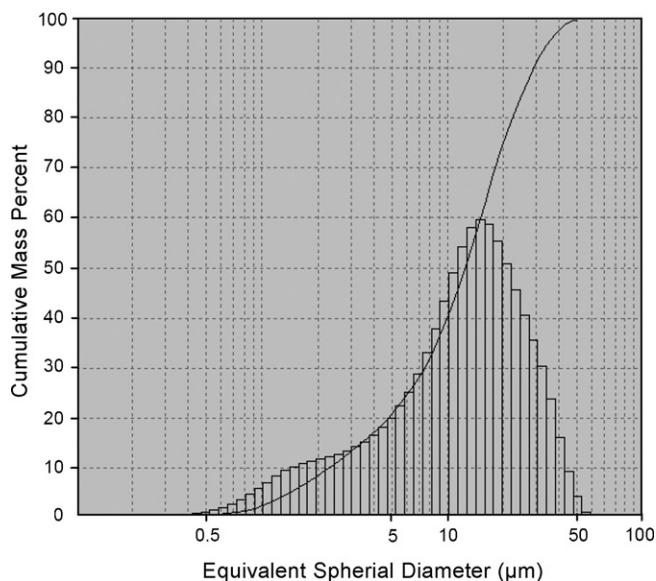


Fig. 1. Particle size distribution of the mica glass powder.

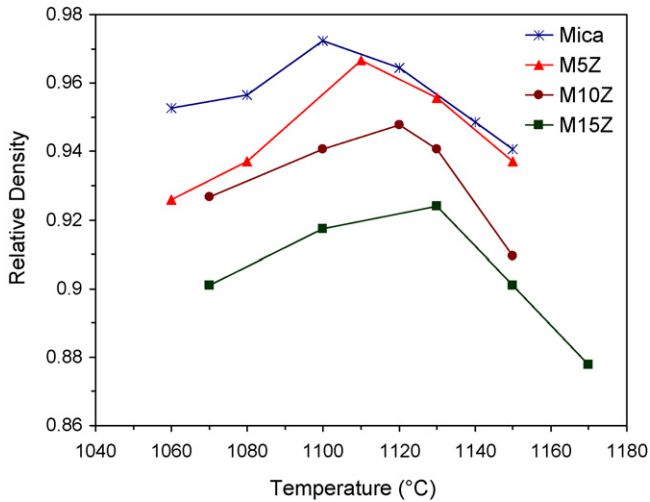


Fig. 2. Relative density of fired samples vs. temperature.

tetragonal zirconia ($t\text{-ZrO}_2$) and minor amount of zircon (ZrSiO_4) were detected in the composites. The content of $t\text{-ZrO}_2$ calculated using Garvie and Nicholson¹⁵ method was 37.6%, 33.6% and 29.6% of the whole content of Y-PSZ in composites M5Z, M10Z and M15Z, respectively.

The as-received Y-PSZ powder contained 80% $t\text{-ZrO}_2$, which decreased to about 65% after mixing with glass powder using a jar-mill. This reduction directly resulted from the stress-induced transformation of $t\text{-ZrO}_2$ to $m\text{-ZrO}_2$ during milling, which has also been reported by Murase and Kato.¹⁶ Further decrease in the content of $t\text{-ZrO}_2$ in the fired composites should be due to the transformation of the $t\text{-ZrO}_2$ to $m\text{-ZrO}_2$ happened during sintering process. The formation of zircon and especially this transformation have been reported to arise from a reaction between the residual glassy phase and zirconia phase during sintering.^{17–19} This reaction also decrease the alloying effect of

Y_2O_3 on the stability of $t\text{-ZrO}_2$ phase, by formation of a glass composition in the $\text{Y}_2\text{O}_3\text{-Al}_2\text{O}_3\text{-SiO}_2$ system.¹⁹ The zirconia dissolution have been also observed, previously in the other glass–ceramic matrix composites reinforced with zirconia.^{20–22}

The morphology of the as-received and agglomerated Y-PSZ powder is illustrated in Fig. 4a. In order to investigate the effect of mixing on the degree of dispersion of Y-PSZ particles in the composites, prepared mixture of glass powder and 10 wt.% Y-PSZ (M10Z) was heated to the sintering temperature and then immediately cooled. The back-scattered SEM micrograph of this sample is shown in Fig. 4b. As it can be seen, agglomerated Y-PSZ particles are broken into the very fine particles (less than $1\ \mu\text{m}$), and very well dispersion of particles in the glass matrix is achieved before the completion of sintering process.

The SEM images of the sintered specimens etched with 5 wt.% HF solution for 45 s are illustrated in Fig. 5. Microstructure of the Mica contained plate-like mica crystals with conventional interlocking structure (Fig. 5a). In the M5Z, both fine dispersed particles ($\sim 0.1\ \mu\text{m}$) and agglomerated particles of zirconia were observed (Fig. 5b). Agglomeration became clearer in the M10Z and M15Z (Fig. 5c and d).

By considering the very well dispersion of the Y-PSZ in the glass powder before the commencement of the sintering process (Fig. 4b), and comparing it with the microstructure of the sintered bodies (Fig. 5), it seems that during sintering process, Y-PSZ particles begin to agglomerate between the glass powders,

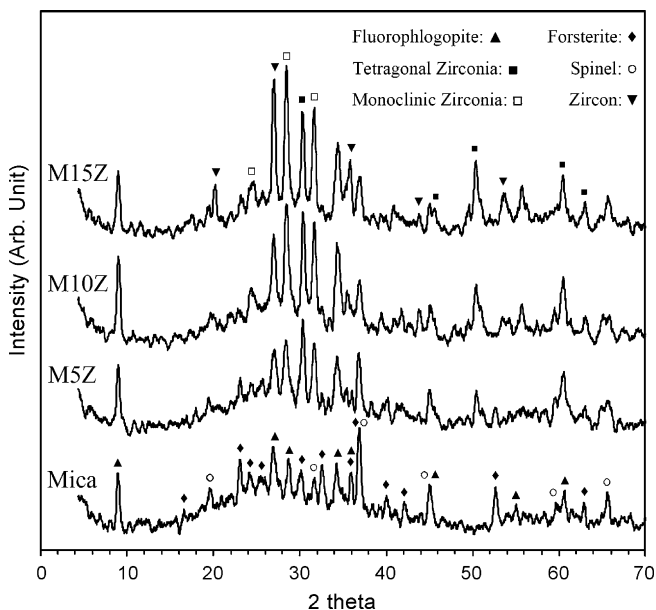


Fig. 3. XRD patterns of sintered specimens.

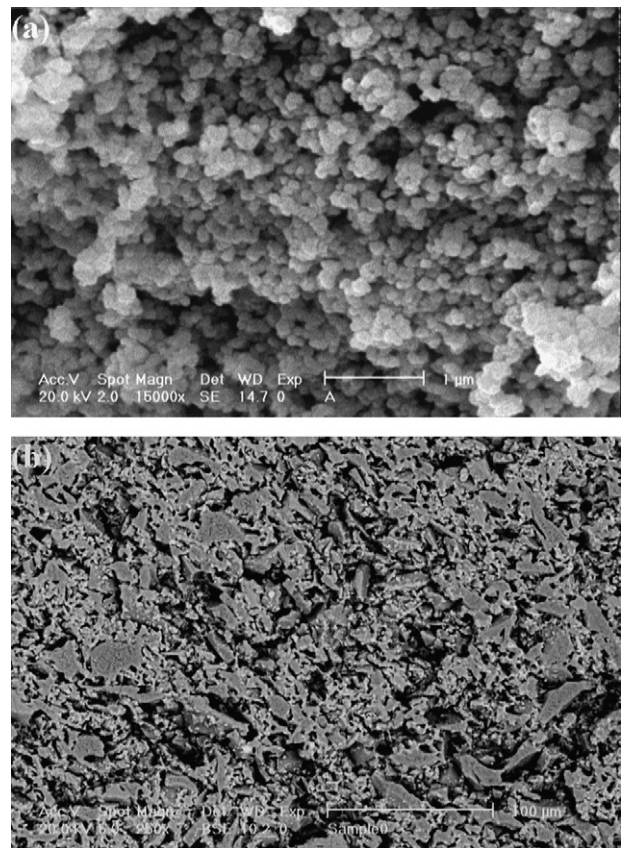


Fig. 4. Morphology of Y-PSZ powder: (a) as-received powder (15,000 \times); (b) dispersed Y-PSZ in the glass powder before the commencement of sintering process (250 \times).

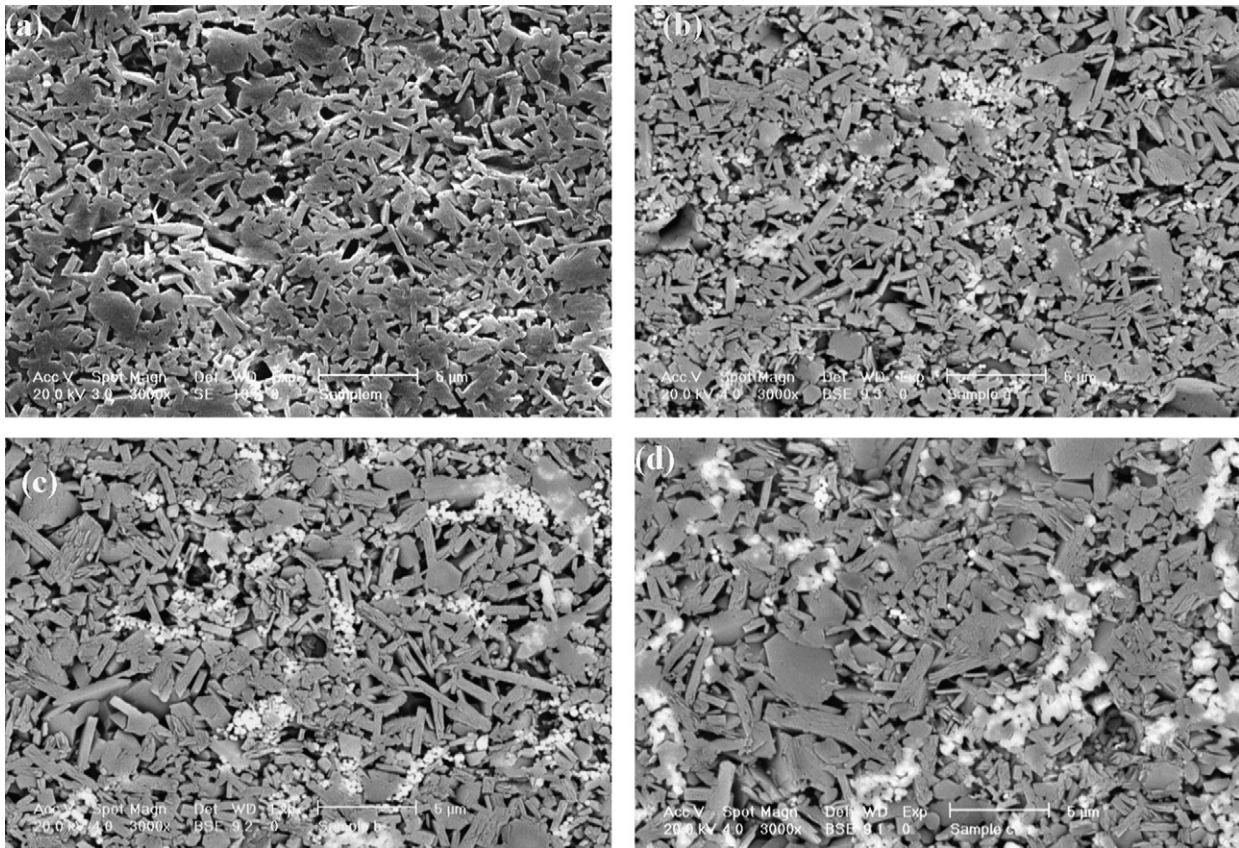


Fig. 5. Microstructures of the sintered samples (3000 \times): (a) Mica, (b) M5Z, (c) M10Z and (d) M15Z.

in order to reduce their free surface energy. The low viscosity of residual glass facilitates the agglomeration of zirconia particles. Furthermore, above-mentioned results show that ZrO_2 particles dissolve to some extent in the residual glass, and subsequently zircon precipitates during the final stage of sintering. This partially dissolution reduces the alloying effect of Y_2O_3 on the stability of $t-ZrO_2$, and so encourages the transformation of $t-ZrO_2$ to $m-ZrO_2$. The transformation of $t-ZrO_2$ to $m-ZrO_2$ during cooling at about $950^\circ C$ is also possible; since the residual glass at this temperature is not rigid enough to retain $t-ZrO_2$ in the matrix. By increasing the content of Y-PSZ in the composites, higher amount of $t-ZrO_2$ transformed to the $m-ZrO_2$. This could be due to an increase in the sintering temperatures, which intensifies the dissolution of Y-PSZ.

Mechanical properties as well as relative density of the sintered specimens have been summarized in Table 1. All composites had a lower relative density than the mica glass–ceramic (Mica). Micro-hardness increased by increasing the content of ZrO_2 in the specimens, but it represented too much deviation from the average values for M10Z and M15Z which is due to the formation of zirconia agglomerates in these samples. Bending strength (σ_f) of M5Z was almost twice that of the Mica. The M10Z and M15Z represented nearly same values of bending strength, which were the maximum strengths of the composites. A trend similar to the bending strengths was observed for fracture toughness (K_{IC}). M10Z and M15Z showed maximum K_{IC} values. Therefore, by incorporating Y-PSZ particles into the

mica glass–ceramic matrix, in spite of more porosity of samples, their bending strength and fracture toughness increased.

Zirconia particles retard the densification of composites due to (i) the dissolution of ZrO_2 which leads to increase the viscosity of residual glass and interferes with further densification of composites and (ii) induction a circumferential tensile stresses which act opposite of viscous flowing of glass matrix.²³

The following mechanisms may be contributed to the reinforcing effect of zirconia particles in the matrix:

- Crack deflection by dispersion strengthening. Crack deflection could occur by mica crystals or dispersed zirconia particles. Fig. 6 shows a detail of a polished cross section of the M10Z composite after Vickers indentation, which a crack propagates from the indent corner. The crack was deviated toward the zirconia agglomerate and propagated across it.
- Transformation toughening by existing $t-ZrO_2$ phase. Several criteria are necessary before transformation toughening can be achieved by addition of partially stabilized ZrO_2 particles to a host matrix: (1) ZrO_2 particles not dissolved by host; (2) particle size of ZrO_2 typically under $0.5 \mu m$; (3) host microstructure strong enough to retain ZrO_2 particles in the tetragonal form during cooling; (4) the amount of retained $t-ZrO_2$ in the matrix.^{13,14}

In this study, it seems that transformation toughening has a little contribution to the increase of fracture toughness,

Table 1
Mechanical properties and relative density of specimens

Sample	Vickers micro-hardness (GPa)	Bending strength, σ_f (MPa)	Fracture toughness, K_{IC} (MPa m ^{1/2})	Relative density (%)
Mica	2.62 ± 0.36	50.91 ± 10.5	0.8 ± 0.08	97.2
M5Z	3.04 ± 0.14	103.31 ± 20.46	1.09 ± 0.11	96.6
M10Z	3.83 ± 0.83	131.63 ± 7.77	1.37 ± 0.14	94.7
M15Z	4.35 ± 0.64	132.47 ± 13.8	1.36 ± 0.07	92.4

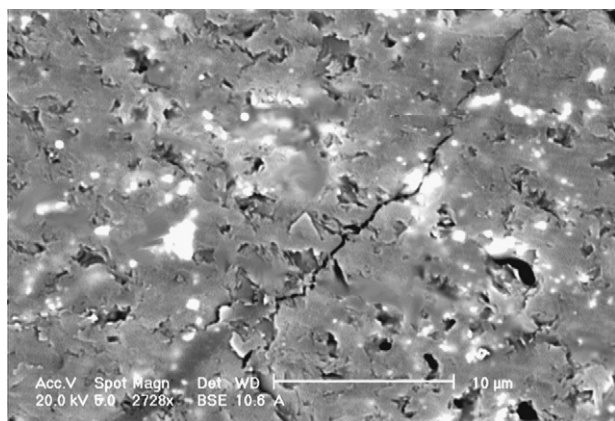


Fig. 6. Crack path induced by Vickers indentation on M10Z composite.

since above-mentioned criteria were not fully satisfied. ZrO₂ particles dissolved in the matrix and t-ZrO₂ transformed to m-ZrO₂. The amount of retained t-ZrO₂ is relatively low for transformation toughening to become dominant mechanism for improving mechanical properties. Also, it seems that the residual glass is not rigid enough at high temperature to retain ZrO₂ particles in the tetragonal form during cooling.

- (c) Dissolution of ZrO₂ in the residual glass. This dissolution incorporates minor amounts of Zr⁴⁺ into the residual glass structure. The presence of Zr ions in the residual glass network, which produce bracing by complex [ZrO₄] structural units,^{8,18} may represent another reinforcement mechanism.

It could be concluded that prevalent mechanism for improving mechanical properties is the crack deflection by dispersion strengthening. High degree of dispersed ZrO₂ particles in M5Z composite resulted in the dramatic increase of strength. But, bending and fracture strength of M15Z is similar to the M10Z, and they represent a little increase in comparison to the M5Z. This can be attributed to the insufficient densification of M15Z and the formation of agglomerated ZrO₂ particles that would reduce the possibility of deflection by second phases.

4. Conclusions

1. Mica glass–ceramic composites toughened by Y-PSZ particles, which have desirable final density and improved mechanical properties, were successfully fabricated via pressureless sintering.
2. The dissolution of Y-PSZ occurred in the residual glass and resulted in the formation of zircon and transformed m-ZrO₂. This dissolution reduces the alloying effect of Y₂O₃ on the

stability of t-ZrO₂, and transformation of t-ZrO₂ to m-ZrO₂ occurs. By increasing the content of Y-PSZ in the composites, higher amount of t-ZrO₂ transformed to the m-ZrO₂.

3. The results showed that crack deflection by mica crystals and dispersed zirconia particles could be a prevalent mechanism for improving mechanical properties, and transformation toughening has a little contribution to the increase of fracture toughness.

References

1. Höland, W. and Beall, G., *Glass–Ceramic Technology*. The American Ceramic Society, Westerville, OH, 2002, pp. 236–240.
2. Chyung, C. K., Beall, G. H. and Grossman, D. G., Microstructures & mechanical properties of mica glass–ceramics. In *Tenth International Congress on Glass. Part II*, ed. M. Kunugi, M. Tashiro and N. Saga. The Ceramic Society of Japan, Japan, 1974, pp. 1167–1194.
3. Uno, T., Kasuga, T. and Nakajima, K., High-strength mica-containing glass–ceramics. *J. Am. Ceram. Soc.*, 1991, **74**, 3139–3141.
4. Cheng, K., Wan, J. and Liang, K., Hot-pressed mica glass–ceramics with high strength and toughness. *J. Am. Ceram. Soc.*, 1999, **82**, 1633–1634.
5. Cheng, K., Wan, J. and Liang, K., Enhanced mechanical properties of orientated mica glass–ceramics. *Mater. Lett.*, 1999, **39**, 350–353.
6. Habelitz, S., Carl, G. and Rüssel, C., Processing, microstructure and mechanical properties of extruded mica glass–ceramics. *Mater. Sci. Eng. A*, 2001, **307**, 1–14.
7. Uno, T., Kasuga, T., Nakayama, S. and Ikushima, A. J., Microstructure of mica-based nanocomposite glass–ceramics. *J. Am. Ceram. Soc.*, 1993, **76**, 539–541.
8. Li, H., You, D., Zhou, C. and Ran, J., Study on machinable glass–ceramic containing fluorophlogopite for dental CAD/CAM system. *J. Mater. Sci. Mater. Med.*, 2006, **17**, 1133–1137.
9. Eftekhari Yekta, B., Hashemi Nia, S. and Alizadeh, P., The effect of B₂O₃, PbO and P₂O₅ on the sintering and machinability of fluoromica glass–ceramics. *J. Eur. Ceram. Soc.*, 2005, **25**, 899–902.
10. Eftekhari Yekta, B., Hashemi Nia, S. and Alizadeh, P., Influence of TiO₂, Cr₂O₃ and ZrO₂ on sintering and machinability of fluorophlogopite glass–ceramics. *Br. Ceram. Trans.*, 2004, **103**, 235–237.
11. Khatib Zadeh, S., Samedani, M., Eftekhari Yekta, B. and Hashemi Nia, S., Effect of sintering and melt casting methods on properties of a machinable fluor-phlogopite glass–ceramic. *J. Mater. Proc. Tech.*, in press.
12. Lynch, C. T., Vahldiek, F. and Robinson, L., Monoclinic–tetragonal transition of zirconia. *J. Am. Ceram. Soc.*, 1961, **44**, 147–148.
13. Hannink, R. H. J., Kelly, P. M. and Muddle, B. C., Transformation toughening in zirconia-containing ceramics. *J. Am. Ceram. Soc.*, 2000, **83**, 461–487.
14. Richerson, D. W., *Modern Ceramic Engineering*. Marcel Dekker, New York, 1992, pp. 731–762.
15. Garvie, R. and Nicholson, P., Phase analysis in zirconia system. *J. Am. Ceram. Soc.*, 1972, **67**, 303–305.
16. Murase, Y. and Kato, E., Phase transformation of zirconia by ball-milling. *J. Am. Ceram. Soc.*, 1979, **62**, 527–527.

17. Choi, S. Y. and Ahn, J. M., Viscous sintering and mechanical properties of 3Y-TZP-reinforced LAS glass–ceramic composites. *J. Am. Ceram. Soc.*, 1997, **80**, 2982–2986.
18. Schweiger, M., Frank, M., Clausbruch, C. V., Höland, W. and Rheinberger, V., Microstructure and properties of a composite system for dental applications composed of glass–ceramics in the $\text{SiO}_2\text{--LiO}_2\text{--ZrO}_2\text{--P}_2\text{O}_5$ system and ZrO_2 -ceramic (TZP). *J. Mater. Sci.*, 1999, **34**, 4563–4572.
19. Claussen, N., Microstructural design of zirconia-toughened ceramics (ZTC). In *Advances in Ceramics, Vol. 12, Science and Technology of Zirconia II*, ed. N. Claussen, M. Rühle and A. H. Heuer. American Ceramic Society, Columbus, OH, 1984, pp. 325–351.
20. Verné, E., Defilippi, R., Carl, G., Vitale Brovarone, C. and Appendino, P., Viscous flow sintering of bioactive glass–ceramic composites toughened by zirconia particles. *J. Eur. Ceram. Soc.*, 2003, **23**, 675–683.
21. Fernandez, C., Verné, E., Vogel, J. and Carl, G., Optimisation of the synthesis of glass–ceramic matrix biocomposites by the “response surface methodology”. *J. Eur. Ceram. Soc.*, 2003, **23**, 1031–1038.
22. Pascual, M. J., Durán, A. and Pascual, L., Sintering behavior of composite materials borosilicate glass– ZrO_2 fibre composite materials. *J. Eur. Ceram. Soc.*, 2002, **22**, 1513–1524.
23. Scherer, G. W., Sintering with rigid inclusions. *J. Am. Ceram. Soc.*, 1987, **70**, 719–725.